

## Use of Experimental Design for the Optimization of the Production of New Secondary Metabolites by Two *Penicillium* Species

Eli F. Pimenta,<sup>†</sup> Aline M. Vita-Marques,<sup>†,△</sup> Aristeu Tininis,<sup>‡</sup> Mirna H. R. Selegim,<sup>§</sup> Lara D. Sette,<sup>⊥</sup> Katyuscya Veloso,<sup>||</sup> Antonio G. Ferreira,<sup>||</sup> David E. Williams,<sup>∇</sup> Brian O. Patrick,<sup>∇</sup> Doralyn S. Dalisay,<sup>∇</sup> Raymond J. Andersen,<sup>∇</sup> and Roberto G. S. Berlinck<sup>\*†</sup>

Instituto de Química de São Carlos, Universidade de São Paulo, CP 780, CEP 13560-970, São Carlos, SP, Brazil, Instituto Federal de Educação, Ciência e Tecnologia, 14169-263, Sertãozinho, SP, Brazil, Departamento de Ecologia e Biologia Evolutiva, Universidade Federal de São Carlos, São Carlos, SP, Brazil, Divisão de Recursos Microbianos, Centro Pluridisciplinar de Pesquisas Químicas, Biológicas e Agrícolas, Universidade Estadual de Campinas, CP 6171, 13083-970, Campinas, SP, Brazil, Departamento de Química, Universidade Federal de São Carlos, São Carlos, SP, Brazil, and Departments of Chemistry and Earth and Ocean Sciences, University of British Columbia, Vancouver, British Columbia, V6T 1Z1, Canada

Received July 9, 2010

A fractional factorial design approach has been used to enhance secondary metabolite production by two *Penicillium* strains. The method was initially used to improve the production of bioactive extracts as a whole and subsequently to optimize the production of particular bioactive metabolites. Enhancements of over 500% in secondary metabolite production were observed for both *P. oxalicum* and *P. citrinum*. Two new alkaloids, citrinalins A (**5**) and B (**6**), were isolated and identified from *P. citrinum* cultures optimized for production of minor metabolites.

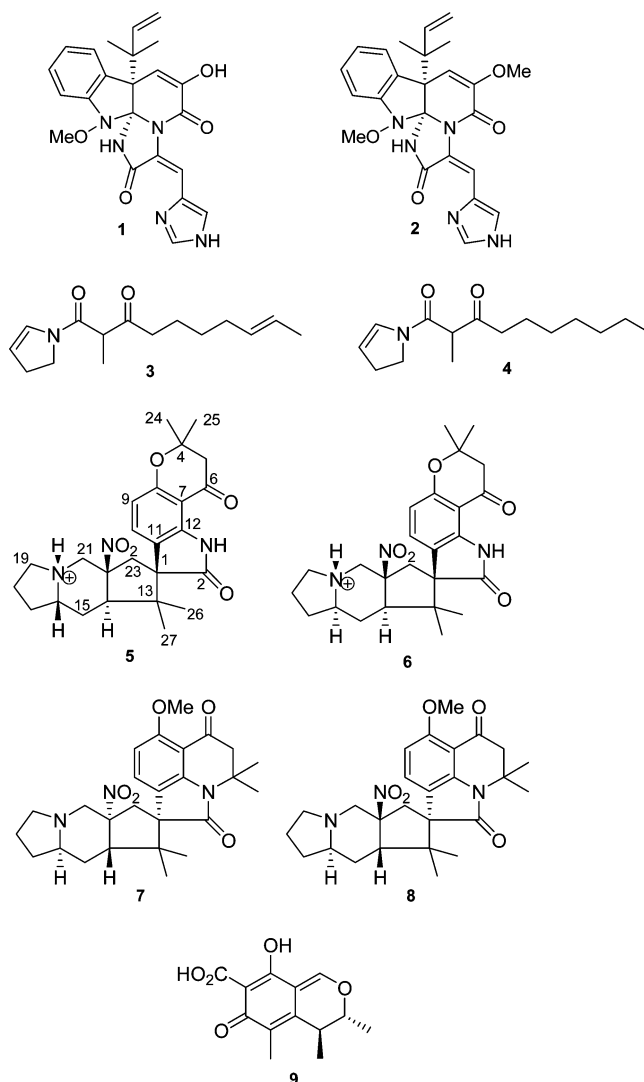
The production of secondary metabolites by fungal strains is of major economic importance in the food, agrochemical, and pharmaceutical industries.<sup>1–3</sup> Many high-profile anti-infective agents, including the well-known penicillins, are fungal secondary metabolites,<sup>4,5</sup> and kojic acid, produced by various *Aspergillus*, *Penicillium*, and *Acetobacter* strains, is widely used in the food industry.<sup>6,7</sup>

Secondary metabolite production by fungal strains is often limited in quantity by a number of factors that affect metabolic turnover. These include the choice of carbon, nitrogen, and phosphorus sources,<sup>1,8,9</sup> pH, temperature, media and saline composition,<sup>8,10</sup> and the use of specific culturing techniques.<sup>11,12</sup> The genetic and enzyme makeup of the producing organism and the involvement of low molecular weight signaling molecules can also play important roles in the regulation of secondary metabolite production.<sup>5,8,13–15</sup>

Several approaches have been proposed to enhance secondary metabolite production by fungal strains. These include strain improvement,<sup>16</sup> optimization of media composition,<sup>17–23</sup> variation of culture conditions,<sup>8,24–27</sup> and microbial coculture.<sup>28–32</sup>

In addition to the variation of culture conditions, the use of statistical models for experimental design also has been reported to optimize fungal growth, biochemical production,<sup>33–36</sup> and biologically active secondary metabolite production.<sup>37–41</sup> While the classical “one-factor-at-a-time” approach requires a large number of univariate experiments to establish the optimal metabolite production conditions,<sup>42,43</sup> multivariate analysis has been successfully applied to the optimization of the production of particular known primary or secondary metabolites.<sup>44</sup> However, no attempts have been made to apply experimental design and multivariate analysis to the relevant problem of increasing the production of

unknown bioactive secondary metabolites in extracts in order to enhance the discovery of new compounds.



\* To whom correspondence should be addressed. Tel: +55-16-33739954. Fax: +55-16-33739952. E-mail: rgsberlinck@iqsc.usp.br.

<sup>†</sup> Universidade de São Paulo.

<sup>△</sup> Current address: Faculdade de Medicina de São José do Rio Preto, Avenida Brigadeiro Faria Lima, 5544, São José do Rio Preto - SP, 15090-000, Brazil.

<sup>‡</sup> Instituto Federal de Educação, Ciência e Tecnologia.

<sup>§</sup> Departamento de Ecologia e Biologia Evolutiva, Universidade Federal de São Carlos.

<sup>⊥</sup> Universidade Estadual de Campinas.

<sup>||</sup> Departamento de Química, Universidade Federal de São Carlos.

<sup>∇</sup> University of British Columbia.

**Table 1.** Range of the Different Parameters Investigated in the Fractional Factorial Design (fFD) Experiments

level	[saline]	[nutrients]	time of incubation (days)	pH	temperature of incubation (°C)
+1	80%	60%	28	8	30
-1	20%	10%	14	6	15

Herein we report the use of a statistical experimental design methodology to improve the growth and secondary metabolite production by two marine-derived fungal strains, *Penicillium oxalicum* and *P. citrinum*, without previous knowledge of the chemical constituents present in their media extracts. This methodology played a critical role in the discovery of the new alkaloids citrinalins A (**5**) and B (**6**), thereby providing proof-of-concept validation for the use of a statistical design approach as a tool to aid bioactive secondary metabolite discovery.

## Results and Discussion

Extracts obtained from the culture media of *P. oxalicum* and *P. citrinum* displayed antimycobacterial activity against *Mycobacterium tuberculosis* H37Rv and cytotoxic activity against HCT-8 colon and B16 murine melanoma cancer cell lines (*P. oxalicum*), as well as antifungal activity against *Candida albicans* ATCC 10231 (*P. citrinum*).<sup>45</sup> When production batches of these two organisms were grown under the same culture conditions used to generate extracts for screening, only very small amounts were obtained. Therefore, we decided to explore the use of experimental design methods for the optimization of secondary metabolite production by both *Penicillium* strains, in order to improve the amounts of the minor bioactive components required for structure elucidation.

Five growth parameters were chosen to investigate on two levels (upper, +1; lower, -1): the total medium saline concentration, the total nutrient concentration, the time of incubation, the pH of the medium, and the temperature of incubation (Table 1). Although many other factors could be considered,<sup>37</sup> the parameters we defined are frequently evaluated for secondary metabolite production by microbial strains.<sup>38,46,47</sup> As the first step, a fractional factorial design (fFD) method was used in order to establish the best conditions from a set of 19 growth experiments (see Experimental Section and Tables S1 and S2 in the Supporting Information) for each *Penicillium* strain. After all growth experiments, each culture medium was subjected to SPE, and the four fractions obtained were analyzed by HPLC. The total chromatogram area for each SPE fraction from each growth experiment was converted to a pure numeral. In parallel, all SPE fractions obtained were weighed. After HPLC analyses, each growth experiment gave a total chromatogram area for each SPE fraction collected, as well as a total chromatogram area/fraction weight ratio. We observed that the total chromatogram area/fraction weight ratio gave a more reliable response for each growth experiment, indicating fractions enriched in secondary metabolites by measuring the increase of the chromatogram area relative to the amount of fraction obtained. The results of the fFD analysis were tabulated and analyzed. After optimal conditions were established, the strains were regrown using the defined optimal conditions to check the increase in secondary metabolite production.

The results of the fFD analysis for the *P. oxalicum* growth experiments indicated the following optimal conditions for enhanced production of fractions 3 (25:75 H<sub>2</sub>O/MeOH) and 4 (100% MeOH) obtained from the SPE of the liquid media of all growth experiments: (a) 20% of the original saline concentration; (b) 10% or 60% of the original nutrient concentration; (c) time of growth: 14 days; (d) pH 6.0 or 8.0; (e) temperature of growth: 30 °C. These results indicated that nutrient concentration and medium pH were unimportant parameters for the enhancement of secondary metabolite production by *P. oxalicum*.

After the statistical analysis, two new growth experiments of *P. oxalicum* were performed (five replicates of each) using the optimized conditions F30-OPTIMUM-1 and -2, as shown in Table 2. Integration of the chromatogram area obtained from the HPLC analyses (10 to 25 min) and the weight of the SPE fractions generated using the optimal growth conditions were compared with the chromatogram areas and the weight of SPE fractions generated after *P. oxalicum* growth under the standard conditions (three replicates). These results are shown in Table 2, which presents the ratio between the average values of the HPLC chromatogram areas and the weight of each SPE fraction for all of the five replicate growth experiments using each of the two optimal conditions. While the absolute values of the average weight of the SPE fractions, as well as of the average chromatogram areas, recorded for the optimized experiments are smaller than the corresponding average values of the triplicate experiments performed under standard conditions, the ratios between chromatogram area/fraction weight are significantly higher. These results show that there has been a significant increase in the total metabolite production over the total weight of the SPE fractions; that is, the fractions obtained were significantly enriched in secondary metabolites. In the case of the SPE-F3, the condition F30-OPTIMUM-2 gave the largest chromatographic area of secondary metabolites (enhancement of 2.18-fold), while the condition F30-OPTIMUM-1 gave the best enhancement of the chromatographic area/fraction weight relationship. In the case of the SPE-F4, the growth condition F30-OPTIMUM-1 gave a remarkable 5.3-fold enhancement of the chromatogram area/fraction weight relationship. The results clearly indicated that the optimization method was successful at increasing the overall secondary metabolite production by *P. oxalicum*.

The SPE-F3 obtained from *P. oxalicum* grown under F30-OPTIMUM-2 conditions contained metabolites with HPLC retention times between 16 and 21 min (Figure 2a and b). Fractions 1 (75:25 H<sub>2</sub>O/MeOH) and 2 (1:1 H<sub>2</sub>O/MeOH) contained mainly very polar compounds related to amino acids, sugars, and other compounds from the growth medium and were not further analyzed. Fraction SPE-F4 contained small amounts of the same compounds present in fraction 3. Therefore, we decided to focus on the analysis of compounds present in fraction 3. LC-PDA-ESIMS analysis of peaks at 17.0 and 20.0 min indicated practically identical UV spectra for both ( $\lambda_{\max}$  202, 224–226, and 326 nm), as well as quasi-molecular ion peaks  $[M + H]^+$  at  $m/z$  434.5 and 448.6, respectively. A search of SciFinder and the Dictionary of Natural Products suggested that the peak at 17.0 min corresponded to melegriene (**1**), and the peak at 20.0 min corresponded to oxaline (**2**).<sup>48</sup> In order to confirm these assignments, seven 250 mL cultures of *P. oxalicum* were regrown using the condition F30-OPTIMUM-2 (Table 2). Solid-phase extraction of the combined medium (1750 mL), as previously described, resulted in 27 mg of fraction 3, which was purified using isocratic C<sub>18</sub> HPLC (eluent: 6:4 MeOH/H<sub>2</sub>O), to give 1.8 mg of melegriene (**1**) and 2.8 mg of oxaline (**2**). The compounds were identified by analysis of their LC-ESIMS and <sup>1</sup>H and <sup>13</sup>C NMR data.<sup>49–52</sup> Oxaline (**2**) is a potent cytotoxic agent that promotes the arrest of the cell cycle at the G<sub>2</sub>/M phase, disrupts the cytoplasmic microtubule assembly, and inhibits the polymerization of microtubule proteins and purified tubulin.<sup>53</sup> Therefore, oxaline (**2**) probably accounts for the cytotoxic activity observed for the extract of *P. oxalicum*. Although *P. oxalicum* medium extract displayed antimycobacterial activity against *M. tuberculosis* H37Rv, oxaline was inactive in this assay.

After the identification of the major metabolite produced by *P. oxalicum* as oxaline (**2**), we examined the enhancement of its production using the optimized conditions. We measured the area of the oxaline peak in the chromatograms generated from the HPLC analysis of each fraction 3 obtained after the SPE of each growth experiment, under standard and optimized conditions. The optimized growth experiments resulted in an enhancement in the ratio of

**Table 2.** *P. oxalicum* (F30) Optimal Growth Conditions Resulting from fFD Analysis Using the Chromatogram Area/SPE Fraction Weight Ratios as Response

growth condition	growth parameters					total chromatogram area/fraction weight	
	[saline]	[nutrients]	time (days)	pH	temperature (°C)	SPE-F3	SPE-F4
standard condition <sup>a</sup>	100%	100%	7	5.8	25	0.148	0.0006
F30-OPTIMUM-1 <sup>b</sup>	20%	10%	14	6	30	0.425	0.0032
F30-OPTIMUM-2 <sup>c</sup>	20%	60%	14	8	30	0.322	0.0009

<sup>a</sup> In unchanged MF medium. <sup>b</sup> Growth condition established by fFD measuring the chromatogram area/fraction weight relationship. <sup>c</sup> Growth condition established by fFD measuring the chromatogram area of SPE fractions 3 and 4.

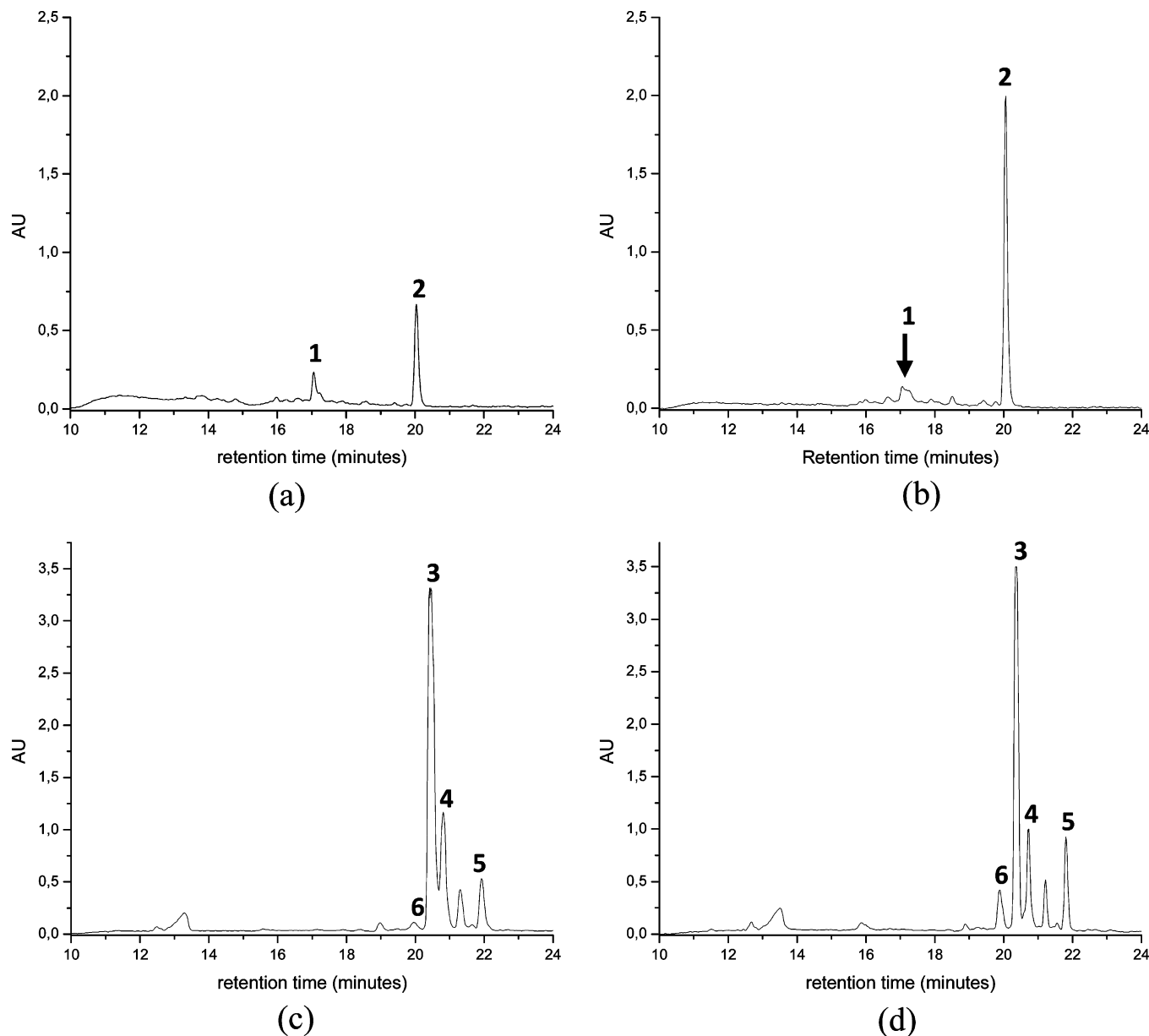


**Figure 1.** HPLC chromatograms generated before and after optimization of growth conditions using experimental design analysis. (a) *Penicillium oxalicum* SPE-F3 obtained using standard growth conditions in unchanged MF medium. (b) *Penicillium oxalicum* SPE-F3 obtained after growth under F30-OPTIMUM-2 conditions. Peak assignments: 1, meleagrine (1); 2, oxaline (2). (c) *Penicillium citrinum* SPE-F4 obtained under standard growth conditions in unchanged MF medium. (d) *Penicillium citrinum* SPE-F4 obtained after growth under F53-OPTIMUM-3 conditions. Peak assignments: 3, compound 3; 4, compound 4; 5, citrinalin A (5); 6, citrinalin B (6). HPLC conditions: see Experimental Section.

oxaline peak area/fraction 3 weight of almost 500% when compared to the standard growth conditions in the MF medium (Table 3). The results clearly indicated that the optimized production of *P. oxalicum* metabolites could be performed with no previous knowl-

edge of their structures, in order to obtain larger quantities of the metabolites for further structure elucidation and biological evaluation.

The same statistical analysis used for *P. oxalicum* was applied in the optimization of growth and production of secondary

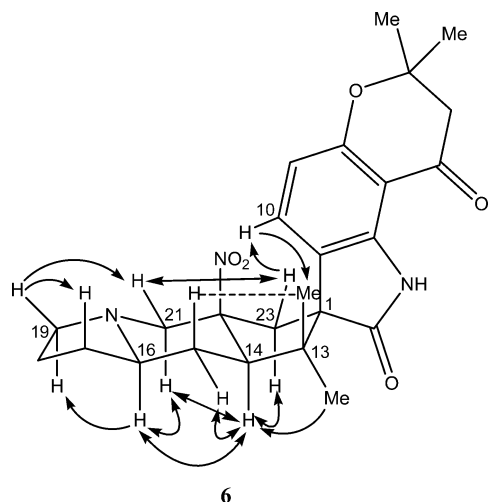


**Figure 2.** NOE couplings observed for citrinalin B (**6**) in the tROESY spectrum. The dashed line indicates a very weak NOE effect.

**Table 3.** Enhancement of Oxaline Production by *P. oxalicum* Using Optimized Conditions by Measuring Oxaline (**2**) Peak Area/SPE Fraction 3 Weight Ratio<sup>a</sup>

growth condition	oxaline ( <b>2</b> ) peak area/fraction 3 weight	increase in the oxaline peak area (%)	increase in oxaline peak area/fraction 3 weight (%)
standard condition	0.022		
F30-OPTIMUM-1	0.1207	25	450
F30-OPTIMUM-2	0.127	155	477

<sup>a</sup> HPLC chromatogram peak (Figure 1b):  $t_R = 20.0$  min.

metabolites by *P. citrinum*. The results of fFD analysis indicated three optimal conditions (F53-OPTIMUM-1, -2, and -3) for enhanced production of all fractions obtained after SPE of the liquid media (Table 4): (a) 20% of the original saline concentration; (b) 10% or 60% of the original nutrient concentration; (c) time of growth: 14 days; (d) pH 6.0 or 8.0; (e) temperature of growth: 15 or 30 °C.

As with *P. oxalicum*, three new growth experiments were performed with *P. citrinum* (five replicates of each) using the optimized conditions as shown in Table 4 (F53-OPTIMUM-1 to -3). The integration of the chromatogram area from the HPLC analyses and the weight of the SPE fractions generated using the optimal growth conditions were compared with those generated after *P. citrinum* growth in the standard conditions in MF medium. We measured both the increase of the total chromatogram area and of the ratio between the chromatogram area/fraction weight to evaluate the improvement in secondary metabolite production by *P. citrinum*, using each of the three growth experiments under optimal conditions (Tables 4–6). The condition F53-OPTIMUM-1 promoted an increase in the production of fraction F3 from the SPE (3.8-fold increase in the chromatogram area/fraction weight ratio, Table 4), while the growth condition F53-OPTIMUM-3 generated a 2.38-fold increase in production of fraction 4 from the SPE measured by the chromatogram area/fraction weight ratio, relative to the growth under standard conditions (Table 4). Therefore, as for *P. oxalicum*, the optimization protocol successfully enhanced the overall secondary metabolite production by *P. citrinum*.

Five peaks were observed in the HPLC analyses of fractions obtained from the optimal growth experiments of *P. citrinum*. These peaks (Figure 1d,  $t_R$  20.0, 20.4, 20.7, 21.2, and 21.9 min) were detected in the chromatograms of SPE-F3 and SPE-F4. The peaks were particularly noticeable in SPE-F4 and appeared with variable intensity depending on the optimal growth conditions used. The optimization analysis was further performed for peaks between 20.4

and 21.9 min by measuring the peak area and also the ratio between the peak area/fraction 4 weight. These results are shown in Tables 5 and 6. Table 5 shows the increase of the area for these peaks of the HPLC chromatograms relative to the corresponding peaks observed in SPE-F4 obtained from *P. citrinum* grown in the standard and optimized conditions. No increase for the area of the peaks at  $t_R$  20.4 and 20.7 min is observed for any of the three optimal growth conditions. A significant increase (351%) in the area of the peak at  $t_R$  21.2 min was observed using the growth condition F53-OPTIMUM-2, while an increase of 90% in the area of the peak at  $t_R$  21.9 min was found using the F53-OPTIMUM-3 condition. Therefore, it was clear that the production of each of the four different compounds by *P. citrinum* required distinct optimal conditions. However, analysis of the peak area/fraction weight ratios showed that F53-OPTIMUM-3 (Table 6) was generally a superior growth condition for the production of secondary metabolites.

LC-PDA-ESIMS analysis of the peaks at  $t_R$  20.4, 20.7, and 21.2 min indicated nearly identical UV spectra for all ( $\lambda_{max}$  243 nm). The MS analysis of these peaks showed  $[M + H]^+$  signals at  $m/z$  250.2, 252.6, and 252.6, while the corresponding  $[M + Na]^+$  signals were observed at  $m/z$  272.3, 274.4, and 274.4, respectively. A search of SciFinder and the Dictionary of Natural Products suggested that the peak at 20.4 min corresponded to (*E*)-1-(2,3-dihydro-1*H*-pyrrol-1-yl)-2-methyldec-8-ene-1,3-dione (**3**) and the peak at 21.2 min corresponded to 1-(2,3-dihydro-1*H*-pyrrol-1-yl)-2-methyldecane-1,3-dione (**4**).<sup>54–56</sup> These assignments were confirmed after a new growth of *P. citrinum* using the condition F53-OPTIMUM-3 (Table 4) in 2 L of culture medium. This condition was selected because it indicated a higher ratio between the total chromatogram area/weight of HPLC peaks observed for SPE-F4 (Table 6). Solid-phase extraction of the whole medium (2 L) resulted in 160 mg of fraction 3 and 37 mg of fraction 4. Both fractions were purified using isocratic  $C_{18}$  HPLC (eluent: 6:4 MeOH/H<sub>2</sub>O) to give 46 mg of compound **3** and 3.0 mg of **4**. These compounds were identified by analysis of LCESIMS and <sup>1</sup>H <sup>13</sup>C, <sup>1</sup>H–<sup>1</sup>H COSY, HSQC, and HMBC NMR data, as well as by comparison with literature data.<sup>54–56</sup> The identity of the peak at  $t_R$  20.7 min has not yet been established. Compounds **3** and **4** have been previously isolated from *P. brevicompactum* and found to have antifungal, insecticidal, and anti-juvenile hormone activities and probably accounts for the anti-*Candida albicans* activity of *P. citrinum* medium extract.<sup>54–56</sup>

Interestingly, the compounds eluting at 20.0 and 21.9 min with UV absorptions at  $\lambda_{max}$  206, 228, 259, 281 (shoulder), and 356 nm had a completely different UV profile than compounds **3** and **4**. LC-ESIMS analysis of these peaks indicated identical quasi-molecular ions  $[M + H]^+$  at  $m/z$  454.1. After the regrowth of *P. citrinum* in 2 L using the F53-OPTIMUM-3 condition, a small amount of the compound corresponding to the peak at  $t_R$  21.8 min was obtained (less than 1 mg). Reanalysis of the data collected from fFD analysis for the peak at 21.8 min indicated that the only requirements for its enhanced production were a slightly poorer nutrient medium (10% nutrient concentration), a longer incubation time (28 days), and a lower initial pH (6.0) than that used in the optimal condition F53-OPTIMUM-3. Therefore, we decided to regrow *P. citrinum* in a total volume of 2 L using these new growth conditions (F53-OPTIMUM-4).

After the growth, filtration, and SPE using the same conditions as for the previous growth experiments, fractions 3 (25%:75% H<sub>2</sub>O/MeOH) and 4 (100% MeOH) were analyzed by HPLC-PDA-MS, looking for the metabolite at 21.8 min. Using HPLC to guide the large-scale purification, we obtained 1.2 mg of this metabolite, which was the new indole alkaloid citrinalin A (**5**). A minor analogue, citrinalin B (**6**), that eluted at  $t_R$  20.0 min in the HPLC-PDA-MS analysis (Figure 2c and d) was also obtained in less than 1 mg.

**Table 4.** Growth Conditions, HPLC Analysis, and SPE Fraction Weights for *Penicillium citrinum* (F53) Growth Experiments

growth experiment	growth parameters					total chromatogram area/fraction weight	
	[saline]	[nutrients]	time (days)	pH	temperature (°C)	SPE-F3	SPE-F4
standard condition <sup>a</sup>	100%	100%	7	5.8	25	0.1690	0.6587
F53-OPTIMUM-1 <sup>b</sup>	20%	10%	14	8	30	0.6428	0.9599
F53-OPTIMUM-2 <sup>c</sup>	20%	60%	14	6	15	0.1597	0.2204
F53-OPTIMUM-3 <sup>d</sup>	20%	60%	14	8	30	0.1907	1.5721

<sup>a</sup> In unchanged MF medium. <sup>b</sup> Growth condition established by fFD measuring the chromatogram area/fraction weight relationship. <sup>c</sup> Growth condition established by fFD measuring the chromatogram area of SPE fraction 3. <sup>d</sup> Growth condition established by fFD measuring the chromatogram area of SPE fraction 4.

**Table 5.** Variation in the Amount (HPLC peak area) of Secondary Metabolites Produced by *Penicillium citrinum* (F53) in Distinct Growth Experiments<sup>a</sup>

growth experiment	variation in the amount of secondary metabolites produced							
	peak 1 area	% increase	peak 2 area	% increase	peak 3 area	% increase	peak 4 area	% increase
standard condition	0.6749		0.2306		0.0735		0.0831	
F53-OPTIMUM-1	0.1259	-81	0.0179	-92	0.0308	-58	0.0517	-37
F53-OPTIMUM-2	0.5034	-25	0.1838	-20	0.3313	351	0.0184	-77
F53-OPTIMUM-3	0.4849	-28	0.1284	-44	0.0644	-12	0.1582	90

<sup>a</sup> HPLC chromatogram peaks (Figure 1d): peak 1  $t_R = 20.4$  min; peak 2  $t_R = 20.7$  min; peak 3  $t_R = 21.2$  min; peak 4  $t_R = 21.9$  min.

**Table 6.** Variation in the Amount (HPLC peak area/SPE fraction 4 weight) of Secondary Metabolites Produced by *Penicillium citrinum* (F53) in Distinct Growth Experiments<sup>a</sup>

growth experiment	variation in the amount of secondary metabolites produced							
	peak 1 area/weight F4	% increase	peak 2 area/weight F4	% increase	peak 3 area/weight F4	% increase	peak 4 area/weight F4	% increase
standard condition	0.2911		0.0992		0.0316		0.0358	
F53-OPTIMUM-1	0.2325	-20	0.0324	-67	0.0556	76	0.0957	167
F53-OPTIMUM-2	0.1025	-65	0.0378	-62	0.0681	116	0.0038	-89
F53-OPTIMUM-3	0.4732	63	0.1279	29	0.0669	112	0.1703	376

<sup>a</sup> HPLC chromatogram peaks (Figure 2d): peak 1  $t_R = 20.4$  min; peak 2  $t_R = 20.7$  min; peak 3  $t_R = 21.2$  min; peak 4  $t_R = 21.9$  min.

Citrinalin A TFA salt (**5**) gave a  $[M + H]^+$  at  $m/z$  454.2362 in the HRESIMS spectrum, corresponding to a molecular formula of  $C_{25}H_{32}N_3O_5$ , requiring 12 sites of unsaturation. Analysis of its  $^{13}C$  NMR spectrum identified two carbonyl groups, four quaternary  $sp^3$  carbons, two  $sp^2$  methine groups, four quaternary  $sp^2$  carbons, two  $sp^3$  methines, six methylenes, and four methyls.

The presence of a 1,2,3,4-tetrasubstituted benzene moiety was evident from the analysis of COSY and HMBC data. COSY correlations observed between the  $sp^2$  methines at  $\delta_H$  6.61 ( $\delta_C$  109.6, CH-9) and  $\delta_H$  7.34 ( $\delta_C$  132.4, CH-10) were assigned to an *ortho*-coupling ( $J = 8.3$  Hz) between H-9 and H-10. Both H-9 and H-10 showed long-range HMBC correlations (LRCs) to the aromatic carbons at  $\delta_C$  158.8 (C-8) and 105.2 (C-7), while H-9 showed a LRC to the aromatic carbon at  $\delta$  120.9 (C-11) and H-10 showed a  $^3J$  coupling to the aromatic carbon at  $\delta_C$  142.6 (C-12). The presence of an oxidized isopentane moiety attached to C-7 and C-8 was assigned as follows. The hydrogen H-9 showed a LRC to the carbonyl group at  $\delta_C$  192.6 (C-6). A methylene group represented by an AB system at  $\delta_H$  2.84 and 2.75 also showed a LRC to the same carbonyl group, along with correlations to the aromatic carbon C-7, to an oxygen-substituted  $sp^3$  quaternary carbon at  $\delta_C$  79.3 (C-4), and to the methyl groups at  $\delta_C$  25.8 (Me-24) and 26.5 (Me-25). Both Me-24 and Me-25 methyl groups showed LRCs to the methylene  $CH_2$ -5 ( $\delta_C$  48.0) and to C-4. These correlations enabled us to establish the presence of a  $-O-C(Me)_2-CH_2-CO-$  moiety attached to the benzene residue at C-7 and C-8.

An amide group was shown to be attached to the benzene moiety, as the NH hydrogen at  $\delta_H$  10.35 showed LRCs to the aromatic carbons at  $\delta_C$  142.6 (C-12) and 120.9 (C-11) as well as to the carbonyl group at  $\delta_C$  182.9 (C-2). The presence of a spiro  $sp^3$  quaternary carbon ( $\delta_C$  57.5) attached to the amide carbonyl group and to the aromatic C-11 was deduced by observation of LRCs between the spiro carbon with the amide hydrogen (H-3), with H-10

at  $\delta_H$  7.34, with two methyl groups at  $\delta_H$  0.62 (s, Me-26) and 0.83 (s, Me-27), as well as with H-23a ( $\delta_H$  3.19). Therefore, we established the presence of a 7,7-dimethyl-7,8-dihydropyrano[2,3-g]indole-2,9(1*H*,3*H*)-dione moiety in **5**.

Further analysis of the HMBC spectrum of **5** indicated that both methyl groups Me-26 and Me-27 were attached to a quaternary carbon at  $\delta_C$  46.1 (C-13). Vicinal to this quaternary carbon was a methine group (CH-14), because its hydrogen ( $\delta_H$  2.89) showed a LRC to C-13. This quaternary carbon also showed a LRC to H-23a, one of the two hydrogens of a methylene group, which also showed LRCs to the aromatic carbon at  $\delta_C$  120.9 (C-11), to a quaternary carbon at  $\delta_C$  92.4, and to CH-14 ( $\delta_C$  45.8). These correlations indicated the presence of a cyclopentane ring, comprised of a quaternary  $sp^3$  carbon (C-13) substituted by two methyl groups (Me-26 and Me-27), a quaternary  $sp^3$  spiro carbon (C-1), a methylene group ( $CH_2$ -23), a heteroatom-substituted quaternary carbon (C-22), and a methine group (CH-14). Up to this point, analysis of the COSY spectrum was not very informative, as only geminal  $^1H-^1H$  correlations were observed for the methylene pairs  $CH_2$ -5 and  $CH_2$ -23 and a vicinal correlation was detected between the two aromatic hydrogens H-9 and H-10.

However, analysis of the COSY spectrum proved useful to establish a  $^1H$  spin system starting at the methine CH-14 ( $\delta_H$  2.89) connected to the methylene group  $CH_2$ -15 ( $\delta_H$  2.39 and 1.88), which was sequentially connected to CH-16 ( $\delta_H$  4.19). The deshielded methine (H-16) was coupled to the methylene  $CH_2$ -17 ( $\delta_H$  2.24 and 1.93), which was sequentially connected to another methylene ( $CH_2$ -18,  $\delta_H$  2.19 and 2.05). The  $CH_2$ -18 methylene showed a correlation to a third methylene at  $\delta$  3.50 and 3.24 ( $CH_2$ -19), which was connected to a heteroatom-attached hydrogen at  $\delta_H$  9.41 (NH-20). Analysis of the HMBC spectrum confirmed the spin system between CH-14 and  $CH_2$ -19.

**Table 7.** NMR Spectroscopic Data (600 MHz  $^1\text{H}$ ; 150 MHz  $^{13}\text{C}$ , DMSO- $d_6$ ) for Citrinalin A (**5**) and B (**6**) TFA Salts

position	citrinalin A ( <b>5</b> )		citrinalin B ( <b>6</b> )	
	$\delta_{\text{C}}$ , mult. ( $\delta_{\text{N}}^a$ )	$\delta_{\text{H}}$ (J in Hz)	$\delta_{\text{C}}$ , mult. ( $\delta_{\text{N}}^a$ )	$\delta_{\text{H}}$ (J in Hz)
1	57.5, C		58.3, C	
2	182.9, C		182.4, C	
3	(-242.1), NH	10.35, s	(-241.1), NH	10.10, s
4	79.3, C		79.2, C	
5	48.0, CH <sub>2</sub>	2.84, d (16.6) 2.75, d (16.6)	48.0, CH <sub>2</sub>	2.80, d (16.6) 2.74, d (16.6)
6	192.6, C		192.6, C	
7	105.2, C		104.9, C	
8	158.8, C		158.7, C	
9	109.6, CH	6.61, d (8.3)	108.8, CH	6.53, d (8.3)
10	132.4, CH	7.34, d (8.3)	132.7, CH	7.51, d (8.3)
11	120.9, C		119.5, C	
12	142.6, C		142.8, C	
13	46.1, C		48.7, C	
14	45.8, CH	2.89, dd (14.0, 3.5)	43.9, CH	3.63, d (9.8)
15	19.8, CH <sub>2</sub>	2.39, ddd (14.0, 14.0, 6.1) 1.88, dd (14.0, 3.5)	26.8, CH <sub>2</sub>	1.83, dd (13.5, 3.2) 1.71, m
16	61.1, CH	4.19 nd	61.3, CH	1.92, nd
17	26.1, CH <sub>2</sub>	2.24, m 1.93, m	30.9, CH <sub>2</sub>	1.90, nd 1.22, nd
18	20.0, CH <sub>2</sub>	2.19, m 2.05, m	20.8, CH <sub>2</sub>	1.63, m
19	55.5, CH <sub>2</sub>	3.50 nd 3.24, m	52.9, CH <sub>2</sub>	2.87, m 1.96, ddd (8.9, 8.9, 8.9)
20	(-316.7), NH	9.41, bs	(n.o.), NH	
21	55.4, CH <sub>2</sub>	4.19 nd 3.53, dd (14.0, 10.9)	64.1, CH <sub>2</sub>	3.61, d (12.9) 2.68, d (12.9)
22	92.4, C		94.6, C	
23	41.0, CH <sub>2</sub>	3.19, d (16.3) 2.43, d (16.3)	41.3, CH <sub>2</sub>	2.65, d (15.7) 2.61, d (15.7)
24	25.8, CH <sub>3</sub>	1.38, s	26.0, CH <sub>3</sub>	1.37, s
25	26.5, CH <sub>3</sub>	1.41, s	26.3, CH <sub>3</sub>	1.39, s
26	20.3, CH <sub>3</sub>	0.62, s	22.7, CH <sub>3</sub>	0.69, s
27	23.4, CH <sub>3</sub>	0.83, s	22.9, CH <sub>3</sub>	0.97, s

<sup>a</sup> The  $^{15}\text{N}$  assignments were not calibrated with an external standard. The  $\delta$  value has an accuracy of about 1 ppm in reference to MeNO<sub>2</sub> (0 ppm) and are assigned on the basis of  $^{15}\text{N}$ gHSQC and  $^{15}\text{N}$ rgHMQC correlations; nd, multiplicity not determined due to overlapping signals; n.o., not observed; in the text, a and b denote downfield and upfield resonances respectively of a geminal pair.

After analysis of the COSY spectrum, it remained to insert structural elements corresponding to a H<sub>3</sub>CNO<sub>3</sub> fragment. The COSY and HMBC spectra indicated the presence of a methylene group ( $\delta_{\text{H}}$  4.19 and 3.53) inserted between the heteroatom substituted with the  $^1\text{H}$  at  $\delta_{\text{H}}$  9.41 and the quaternary carbon at  $\delta_{\text{C}}$  92.4. The proton H-21a showed LRCs to C-19 ( $\delta_{\text{C}}$  55.5), C-16 ( $\delta_{\text{C}}$  61.1), and C-14 ( $\delta_{\text{C}}$  45.8), while H-23b showed a LRC to CH<sub>2</sub>-21 ( $\delta_{\text{C}}$  55.4). Additionally, the chemical shifts of the heteroatom-substituted CH-16 ( $\delta_{\text{C}}$  61.1), CH<sub>2</sub>-19 ( $\delta_{\text{C}}$  55.5), and CH<sub>2</sub>-21 ( $\delta_{\text{C}}$  55.4) clearly suggested the presence of a protonated nitrogen ( $^1\text{H}$  at  $\delta$  9.41) between these groups. Because a NO<sub>2</sub> group remained to be assigned, it was positioned attached to the quaternary carbon at  $\delta_{\text{C}}$  92.4. Therefore, the planar structure of citrinalin A was assigned as **5** (IUPAC 7',7',8,8-tetramethyl-5a-nitro-1,2,3,5,5a,6,7',8,8a,8',9,9a-dodecahydro-1'H-spiro[cyclopenta[f]indolizine-7,3'-pyran[2,3-g]indole]-2',9'-dione).

The relative configuration of citrinalin A (**5**) was established by analysis of  $^1\text{H}$  and tROESY NMR spectra, while its absolute configuration was unambiguously determined by X-ray diffraction analysis, after crystallization from MeOH. The X-ray diffraction analysis of **5** provided an ORTEP diagram (Figure S1, Supporting Information)<sup>57</sup> that revealed its absolute configuration as 1*S*, 14*R*, 16*S*, 22*S*.

Citrinalin B TFA salt (**6**) gave a  $[\text{M} + \text{H}]^+$  ion in the HRESIMS spectrum at  $m/z$  454.2354, corresponding to the same molecular formula as citrinalin A (C<sub>25</sub>H<sub>32</sub>N<sub>3</sub>O<sub>5</sub>). Analysis of its  $^1\text{H}$  and  $^{13}\text{C}$  NMR spectra clearly indicated that it corresponded to a stereoisomer of **5**. The NMR assignments for **6** shown in Table 7 were established by analysis of HSQC, COSY, and HMBC spectra.

The relative configuration of citrinalin B (**6**) was determined by analysis of the tROESY spectrum (Figure 2). Dipolar couplings

observed between H-10 ( $\delta_{\text{H}}$  7.51) and H-23a ( $\delta_{\text{H}}$  2.65) and Me-27 ( $\delta_{\text{H}}$  0.97); very weak between Me-27 and H-15a ( $\delta_{\text{H}}$  1.83); between H23a and H-21a ( $\delta_{\text{H}}$  3.61); and between H-19b ( $\delta_{\text{H}}$  1.96) and H-21b and H-17a ( $\delta_{\text{H}}$  1.90) positioned these hydrogen groups at the same face of citrinalin B. On the other hand, NOEs observed between Me-26 ( $\delta_{\text{H}}$  0.69) and H-14 ( $\delta_{\text{H}}$  3.63), between H-14 and H-15b ( $\delta_{\text{H}}$  1.71), H-16 ( $\delta_{\text{H}}$  1.92), H-21a ( $\delta_{\text{H}}$  3.61), and H-23b ( $\delta_{\text{H}}$  2.61); and between H-16 and H-21a placed these protons at the opposite face of citrinalin B. Along with the NOEs observed, significant chemical shift changes were observed for CH<sub>2</sub>-15, CH<sub>2</sub>-17, and CH<sub>2</sub>-21. Therefore, we assumed a chair conformation for the central six-membered ring with a *cis* relationship between H-14 and H-16, in which the nitro group should be in an axial orientation. The NOE data enabled us to propose the relative configuration 1*S*\*, 14*R*\*, 16*R*\*, 22*S*\* for citrinalin B (**6**). Considering that citrinalins A and B presented quite similar specific rotation values and the same signal, we can suggest the absolute configuration of compound **6** as 1*S*, 14*R*, 16*R*, 22*S*.

Citrinalins A (**5**) and B (**6**) are closely related to cyclopiamines A (**7**) and B (**8**), previously isolated from the fungus *P. cyclopium*.<sup>58</sup> The structures of **7** and **8** were established by analysis of spectroscopic data, extensive chemical correlations, and single-crystal X-ray diffraction analysis of **8**. This later alkaloid has also been isolated from *Aspergillus caespitosus*.<sup>59</sup> No biological activity has been reported for either **7** or **8**. Citrinalins A (**5**) and B (**6**) were subjected to different bioassays. Although the *P. citrinum* medium extract was active against *C. albicans*, both **5** and **6** were inactive in antimicrobial tests against *Staphylococcus aureus*, *Escherichia coli*, and *Pseudomonas aeruginosa* (MICs above 32  $\mu\text{g}/\text{mL}$ ), as well as against *Candida albicans* (inactive at 40  $\mu\text{g}$  per disk; the positive control amphotericin B showed a 20 mm zone of

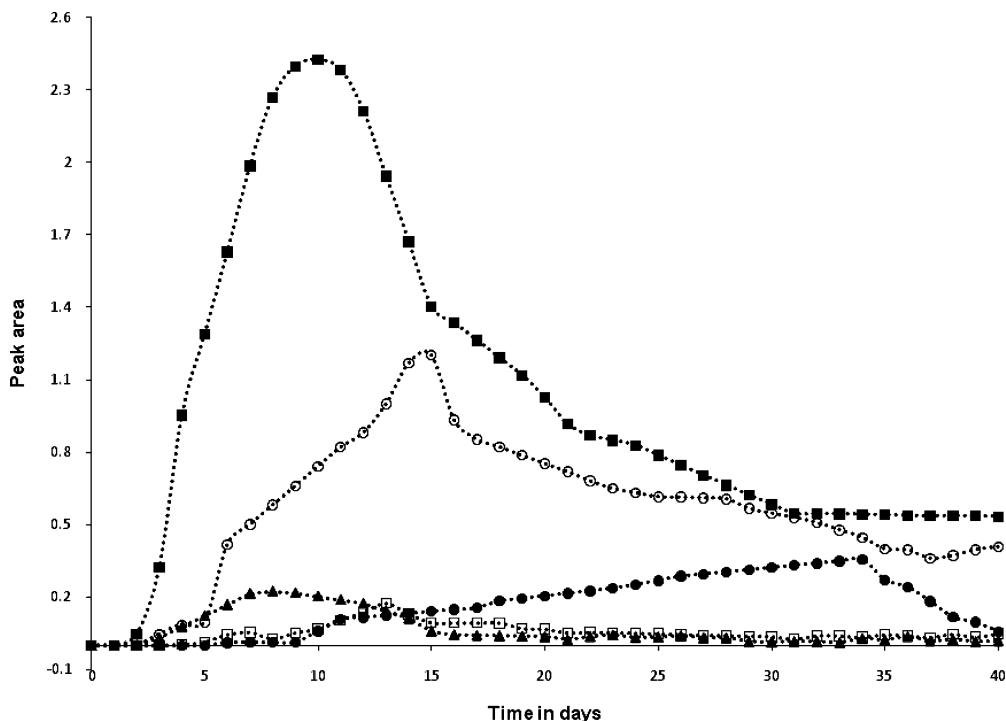


**Figure 3.** Time-course growth experiment of *P. citrinum* ( $n = 2$ ) for the production of compounds **3**, **4**, **5**, **6**, and citrinin (**9**). Plots: □ citrinalin A (**5**); ● citrinalin B (**6**); ○ citrinin (**9**); ■ (*E*)-1-(2,3-dihydro-1*H*-pyrrol-1-yl)-2-methyldec-8-ene-1,3-dione (**3**); ▲ 1-(2,3-dihydro-1*H*-pyrrol-1-yl)-2-methyldecane-1,3-dione (**4**). Growth conditions F53-OPTIMUM-3: [nutrients] = 60%; [ASW] = 20%, pH 8.0, temperature 30 °C. Relative concentrations of alkaloids were measured by integration of HPLC peaks and normalized using the Beer–Lambert law.

inhibition at 8  $\mu\text{g}$  per disk). Both compounds **5** and **6** were also assayed against the HTB-129 breast cancer cell line and showed no cytotoxicity, as their  $\text{IC}_{50}$  values were determined as 174 and 194  $\mu\text{M}$ , respectively (see Experimental Section for bioassay procedures).

After the isolation and identification of compounds **3**–**6** from *P. citrinum*, we decided to perform a two-replicate time course experiment, measuring the relative amount of these metabolites produced by *P. citrinum* F53 during 40 days. The result is shown in Figure 3. The fungus starts the production of the major polyketide **3** at day 2, in significant amounts, with a maximum production at day 11. The biosynthesis of citrinin (**9**) and of the minor polyketide **4** starts at day 3. The concentration of citrinin reaches a maximum at day 15, while the polyketide **4**'s maximal concentration is at day 8. Citrinalin A (**5**) starts to be produced at day 5, with a maximum at day 13, while citrinalin B (**6**) starts to be produced only at day 10, with a maximum at day 34. It is clear that unless the production of alkaloids **5** and **6** is optimized, these can barely be detected relative to the major compounds **3** and **9**. The time-course experiment confirmed the time of incubation for optimized growth experiments observed for *P. citrinum* (Table 4). The increase in the production of compounds **3**, **5**, and **6** by *P. citrinum* by changing from standard conditions to F53-OPTIMUM-3 conditions, respectively, is illustrated in Figure 2c and d. Additionally, Figure 3 shows that at day 14 all metabolites are produced at their maximal individual levels. Therefore, the use of experimental design is highly suitable for the optimization of biosynthesis not only of major metabolites but particularly of the minor ones.

Aiming to obtain larger amounts of citrinalins for their evaluation in biological assays, we have reoptimized the growth conditions of *P. citrinum* for the specific production of these metabolites. A fFD statistical analysis using single-parameter and two-parameter interactions indicated that the lower level of the artificial seawater salts concentration (20%) and the medium pH (6.0) were the most important experimental parameters influencing the production of **5** and **6** (Figure 4). With the help of Figure 4 it is possible to observe that variables 1 (concentration of salts in culture media) and 4 (pH)

show long decreasing arrows and led us to verify that (1) these variables present the highest contrasts and (2) when these variables are in the lowest levels, citrinalins should be produced in higher amounts. It is important to point out that in a  $2^{5-1}$  fractional factorial design the main effects may be confounded with quaternary effects (for example, effect 1 is confounded with 2345; see Figure 4). On the other hand, it is expected that quaternary, tertiary, and secondary effects are lower than the main effects. The observed contrasts for 1 + 2345 (−0.431) and 4 + 1235 (−0.404) have a great contribution from the variables 1 and 4, respectively. The contrast 14 + 235 (0.4654) also showed a high value and may be confounded as either the interaction of variables 1 and 4 (14) or the tertiary effect 235. Thus, we can assume that the effect 235 is small; the contrast 0.4654 has a greater contribution from interaction 14.

Figure 5 shows HPLC analyses of SPE-F4 (100% MeOH) obtained from different growth experiments. Under standard conditions, HPLC analysis indicates that *P. citrinum* produces very small amounts of citrinalin B (**6**) (Figure 5a), but larger quantities of citrinalin A (**5**). Optimized growth conditions shown in Figure 5b and c indicate a larger production of **6** and much lower **5**, in agreement with the time-course experiment (Figure 3), since alkaloid **5** is produced earlier. The best growth condition optimized for the biosynthesis of **6** is shown in Figure 5c, in which the alkaloid is produced in the same relative amounts as the major polyketide **3** (normalized using Beer–Lambert law, relative to  $\epsilon$ ). The growth condition necessary for optimal production of alkaloid **6** is nutritionally very depleted, with only 10% of the original nutrients concentration in the standard MF medium. Quite possibly, this condition promotes significant stress on *P. citrinum*. In the optimal growth condition for **6** it is possible to obtain this metabolite as a major compound, which is barely detected as a minor one using standard growth conditions. This result represents a remarkable output for the change of a metabolic profile of a particular fungal strain, using very simple changes in growth conditions established by experimental design.

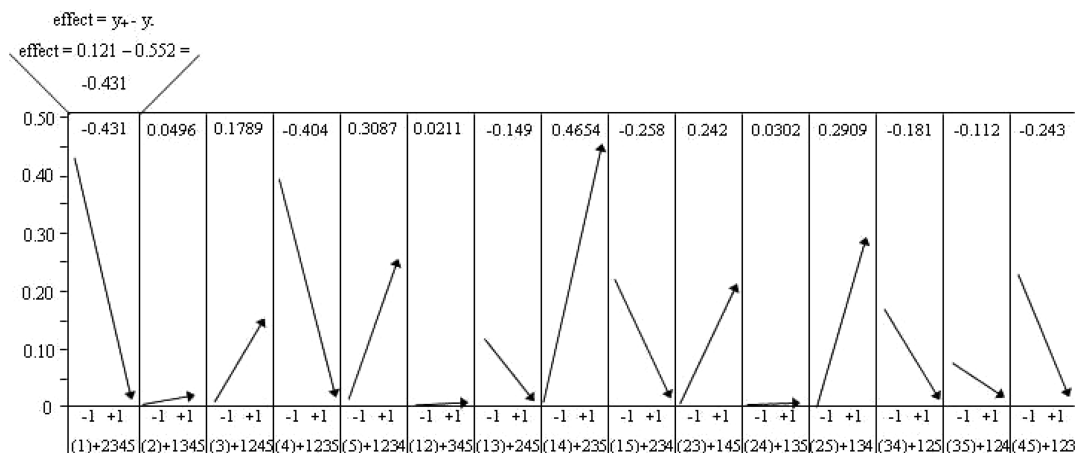


**Figure 4.** Fractional factorial design (FFD)-calculated contrasts of experiments performed for the optimization of *P. citrinum* growth conditions aiming at the optimal production of citrinalin (6). Single-parameter effects are (1) total saline concentration,  $-1 = 20\%$ ,  $+1 = 80\%$ ; (2) total nutrients concentration,  $-1 = 10\%$ ,  $+1 = 60\%$ ; (3) time of incubation,  $-1 = 14$  days,  $+1 = 28$  days; (4) pH,  $-1 = 6.0$ ,  $+1 = 8.0$ ; (5) temperature of incubation,  $-1 = 15$  °C,  $+1 = 30$  °C. Interactions between two growth parameters are indicated as follows: (12) interaction between [salts] and [nutrients], (13) interaction between [salts] and time of incubation, and so on. Arrows indicate the effect of a single growth parameter or of an interaction between two growth parameters on the total chromatogram area of *P. citrinum* metabolites. From upper to lower level, a negative effect. From lower to upper level, a positive effect. Thus, the most important growth parameters influencing the production of citrinalin B (7) by *P. citrinum* are [salts] and pH, and the interaction between them (14) promotes the most significant enhancement.

Analysis of the optimized growth media used for the production of secondary metabolites by *P. oxalicum* and *P. citrinum* indicated a considerable reduction in the saline and nutrients concentration required for both fungal strains. The optimal conditions showed an increase in the time of incubation, from 7 to 14 days for metabolites 1–4 and 5 and up to 28 days for metabolite 6. The optimal pH for secondary metabolite production seemed to be irrelevant for *P. oxalicum*, provided it is in the range between 6.0 and 8.0. The optimal growth temperature of 30 °C was observed for both strains. Once the optimal conditions could be established for secondary metabolite production, five replicates of growth experiments showed excellent reproducibility (data not shown).

The use of experimental design approaches most often leads to the establishment of a single optimal condition for the production of a primary or secondary microbial metabolite.<sup>33,36,38,41–43</sup> However, it is also possible that more than one optimal condition is found for the production of single metabolites.<sup>37,60</sup> In the present investigation, two optimal growth conditions were determined for the production of compounds 1 and 2 by *P. oxalicum*, three optimal growth conditions were established for the production of compounds 3 and 4, and one optimal condition was found for the biosynthesis of 6 by *P. citrinum*. In each case, the increase of metabolite production exceeded 100% compared with growth of both *Penicillium* strains under standard conditions, reaching over 500% enhancement for the production of oxaline (1), showing the power of experimental design to establish optimized conditions for the production of increased amounts of natural products in microbial bioactive extracts.

The optimization method herein reported enables the optimal production of secondary metabolites with no need of preliminary identification. Although we used the HPLC profile and the weight of solid phase extraction fractions as the parameters to be measured for the optimization process, other response parameters can be used, such as the potency of a specific biological activity. The use of experimental design can accelerate the finding of optimal growth conditions for the production of secondary metabolites, in agreement with previously reported related experiments.<sup>41</sup> The reoptimization of growth conditions of a specific bioactive or unknown metabolite can be subsequently performed.

The results herein reported clearly suggest that distinct biosynthetic pathways in *P. citrinum* require distinct optimal growth

conditions. The production of secondary metabolites by fungal strains is quite probably specifically regulated according to optimal growth conditions for gene activation and/or enzymatic activity.

In conclusion, in the present investigation we have shown that the use of experimental design statistical analysis is valid not only for the optimization of a specific metabolite production but also for the production of complex extracts. Such a strategy can be extremely useful in order to generate increased amounts of extracts for further isolation, identification, and biological evaluation of secondary metabolites, particularly for minor metabolites produced in very limited amounts under standard culture conditions.

## Experimental Section

**General Experimental Procedures.** Optical rotations were measured using a Jasco P-1010 polarimeter with sodium light (589 nm). The <sup>1</sup>H and <sup>13</sup>C NMR spectra were recorded on a Bruker AV-600 spectrometer with a 5 mm CPTCI cryoprobe. <sup>1</sup>H chemical shifts are referenced to the residual DMSO-*d*<sub>6</sub> signal ( $\delta$  2.49 ppm), and <sup>13</sup>C chemical shifts are referenced to the DMSO-*d*<sub>6</sub> solvent peak ( $\delta$  39.5 ppm). Low- and high-resolution ESI-QIT-MS spectra were recorded on a Bruker–Hewlett-Packard 1100 Esquire-LC system mass spectrometer. Solvents used for extraction and flash chromatography were glass distilled prior to use. HPLC-grade solvents were utilized without further purification in HPLC separations. HPLC semipreparative separations were performed either with a Waters quaternary pump 600, double beam UV detector 2487, and data module 746 or with a Waters 600E system controller liquid chromatography attached to a Waters 996 photodiode array detector, on which the UV spectra have been recorded as well. HPLC-PDA-MS analyses were performed using a Waters Alliance 2695 coupled online with a Waters 2996 photodiode array detector, followed by a Micromass ZQ2000 mass spectrometry detector with an electrospray interface. The photodiode array scanned the samples at  $\lambda_{\max}$  205 and 254 nm. The mass spectrometer detector was optimized to the following conditions: capillary voltage, 3.00 kV; source block temperature, 100 °C; desolvation temperature, 350 °C, operating in electrospray positive mode; detection range, 200–800 Da with total ion count extracting acquisition. The cone and desolvation gas flow were 50 and 350 L/h, respectively, and were obtained from a Nitrogen Peak Scientific N110DR nitrogen source. Data acquisition and processing were performed using Empower 2.0.

**Microbial Strains.** Strains of *Penicillium oxalicum* F30 and *P. citrinum* F53 have been previously isolated from marine sediments and from a seaweed (*Caulerpa* sp.), respectively.<sup>45</sup> Both *Penicillium* strains were identified by conventional and molecular approaches (see Sup-



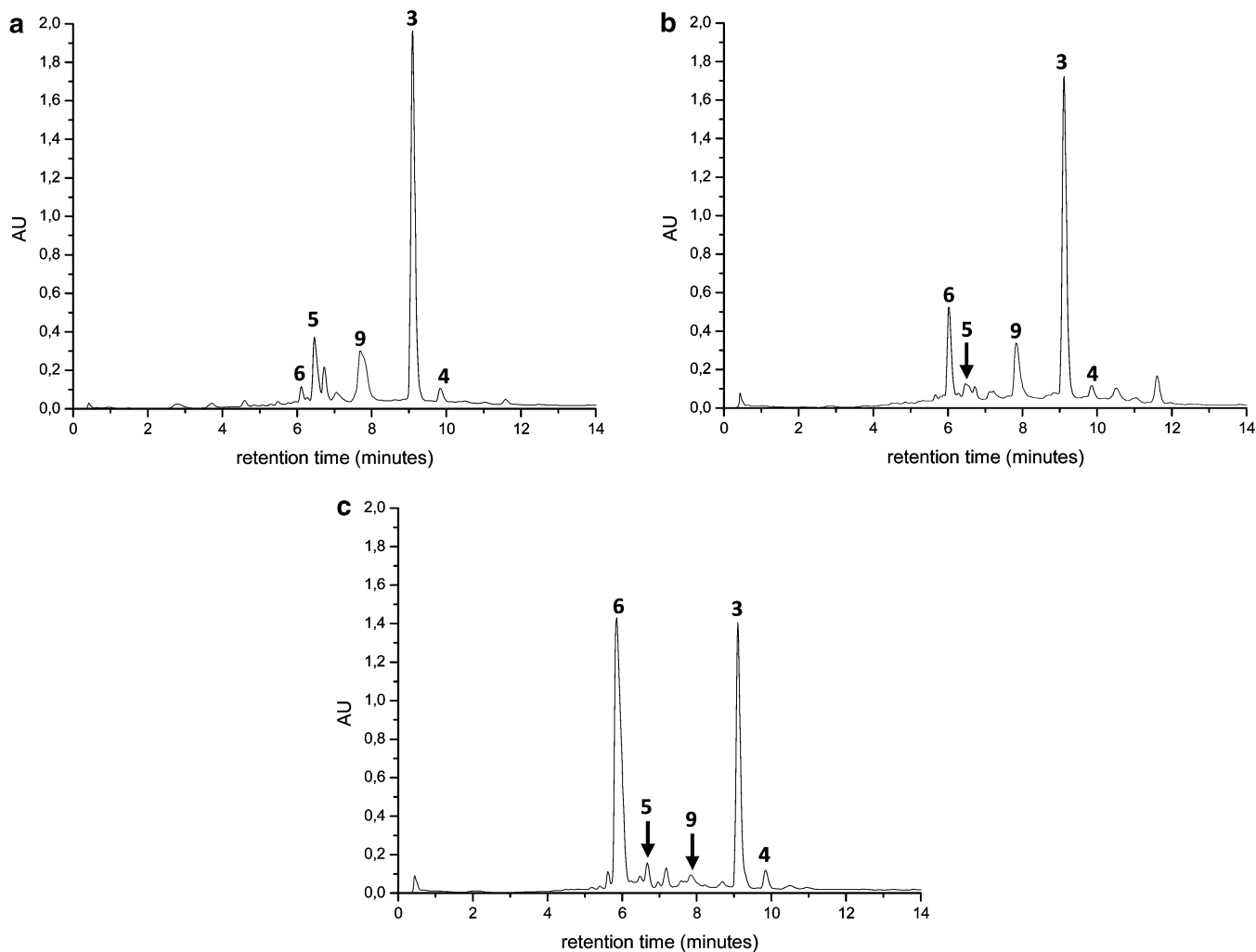


**Figure 5.** (a) HPLC profile of SPE-F2 (100% MeOH) from *P. citrinum* grown in standard conditions (unchanged MF medium). (b) HPLC profile of SPE-F2 (100% MeOH) from *P. citrinum* grown in the following optimal conditions: [nutrients] = 60%, [ASW] = 20%, pH = 8.0, time of incubation = 28 days, temperature = 30 °C. (c) HPLC profile of SPE-F2 (100% MeOH) from *P. citrinum* grown in F53-OPTIMUM-4 conditions: [nutrients] = 10%, [ASW] = 20%, pH = 6.0, time of incubation = 28 days, temperature = 30 °C. HPLC analysis: column, C<sub>18</sub> X-Terra (50 × 2.1 mm; 3.5 μm); eluent, a gradient of 1:1 MeOH/MeCN in H<sub>2</sub>O, starting at 10/90 to 100% 1:1 MeOH/MeCN in 12 min, remaining in the 100% organic solvent mixture until 16 min, then back to the initial conditions after 23 min; flow rate, 0.5 mL/min. PDA at λ<sub>max</sub> 254. Peak assignments: 5, citrinalin A; 6, citrinalin B; 9, citrinin; 3, polyketide 3; 4, polyketide 4.

porting Information). Both *P. oxalicum* F30 and *P. citrinum* F53 strains have been deposited in the CBMAI collection under the accession numbers CBMAI 1185 and CBMAI 1186, respectively.

**Media and Cultivation.** Both strains *P. oxalicum* F30 and *P. citrinum* F53 were grown in 250 mL Erlenmeyer flasks containing standard MF medium: 2% glucose, 1% soluble starch, 2% soytone, 0.5% peptone, 0.03% meat extract, 0.5% yeast extract, agar 1.5% in 100 mL of sterilized artificial seawater (ASW: CaCl<sub>2</sub> 1.36 g/L, MgCl<sub>2</sub> 9.68 g/L, KCl 0.61 g/L, NaCl 30.00 g/L, Na<sub>2</sub>HPO<sub>4</sub> 0.14 mg/L, Na<sub>2</sub>SO<sub>4</sub> 3.47 g/L, NaHCO<sub>3</sub> 0.17 g/L, KBr 100 mg/L, SrCl<sub>2</sub> 40 mg/L, H<sub>3</sub>BO<sub>3</sub> 30 mg/L).

**Experimental Design.** Optimization of growth experiments used fractional factorial design in order to verify which growth parameters affected most fungal growth and the production of secondary metabolites. The growth parameters chosen to be changed were (a) total saline concentration; (b) total nutrients concentration; (c) time of incubation; (d) pH of medium; and (e) temperature of incubation. The parameters were tested at two levels, +1 (higher) and -1 (lower), as defined in Table 1. Details of setting the experimental design experiments are indicated in the Supporting Information. Growth experiments (*n* = 3 for each growth condition) started with the inoculation of 10<sup>5</sup> spores/mL in 50 mL of modified MF medium (according to the experimental design conditions; see the Supporting Information) in 250 mL Schott flasks.

#### Cleanup and HPLC Analysis of Fractions Obtained from the Growth Experiments.

Each of the growth experiments performed under the 16 different growth conditions plus the growth experiments under the average growth conditions 17–19 (Table S2 in the Supporting Information) was processed as follows. At the end of growth, liquid media were filtered through glass wool, in order to separate the mycelia from the liquid media. After filtration, the liquid media (50 mL) were adsorbed onto a C<sub>18</sub> cartridge (2 g). The cartridge was eluted with 100% H<sub>2</sub>O (discarded), H<sub>2</sub>O/MeOH, 75:25 (fraction 1, F1), 1:1 (fraction 2, F2), 25:75 (fraction 3, F3), and 100% MeOH (fraction 4, F4). All fractions obtained after the solid-phase extraction (SPE) of the liquid media from each growth experiment were evaporated to dryness, transferred to vials, and weighed. Aliquots of 1 mg of each fraction obtained from the SPE of the liquid media from each growth experiment were diluted in 1.0 mL of MeOH and analyzed by HPLC with a photodiode array detector monitoring at λ<sub>max</sub> 230 nm, using the following conditions: column, Phenomenex Synergi Fusion RP80 C<sub>18</sub>, 250 × 4.6 mm, 4 μm pore; eluent, a gradient of MeOH in H<sub>2</sub>O, as follows: 100% H<sub>2</sub>O during 1 min, then a linear gradient from 100% H<sub>2</sub>O to 100% MeOH during 25 min, then 5 min at 100% MeOH, then back to 100% H<sub>2</sub>O during 5 min to re-equilibrate to the initial gradient conditions. The HPLC analyses of each SPE fraction gave chromatograms with peaks in the interval between 10 and 25 min. The total area of chromatographic peaks observed in this interval was exported

to Origin Software, integrated, and expressed as pure numerals. After the growth experiments under *a priori* established fFD growth conditions (Table S2, Supporting Information), the results of HPLC analyses of each fraction obtained from each of the 19 growth experiments for both *P. oxalicum* and *P. citrinum*, expressed as pure numerals, were tabulated and compared in order to indicate the larger chromatographic area and the higher chromatographic area/fraction weight ratio as the response of designed experiments. The best results are indicated in Tables 2 and 3 for *P. oxalicum* and in Tables 4, 5, and 6 for *P. citrinum*.

**Isolation of the Main Components Obtained Using Optimal Growth Conditions for *P. oxalicum*.** After optimization of the growth conditions using experimental design, *P. oxalicum* was grown (7 × 250 mL in 500 mL Schott flasks) using the condition F30-OPTIMUM-2 (Table 1). After growth, the liquid media was filtered through a Celite pad and was adsorbed onto a 100% H<sub>2</sub>O-conditioned C<sub>18</sub> reversed-phase cartridge (10 g), using a peristaltic pump (flow rate, 10 mL/min). The column was eluted with 75:25, 50:50, and 25:75 H<sub>2</sub>O/MeOH and 100% MeOH. After evaporation *in vacuo*, fraction 25:75 H<sub>2</sub>O/MeOH presented metabolites **1** and **2**, detected by LC-PDA-MS. This fraction was further purified using a C<sub>18</sub> reversed-phase column (Inertsil ODS-3, 250 × 4.6 mm; 5 μm), using 60:40 MeOH/H<sub>2</sub>O, with a complete run of 30 min and a flow rate of 1.0 mL/min. The major peaks isolated from this separation were identified as oxaline (2.8 mg, **2**) and meleagrine (1.8 mg, **1**) by analyses of <sup>1</sup>H NMR, <sup>13</sup>C NMR, and ESIMS data and comparison with literature data.<sup>49–52</sup>

**Isolation of the Main Components Obtained Using Optimal Growth Conditions for *P. citrinum*.** Using the experimental design results, the growth conditions of *P. citrinum* were established as F53-OPTIMUM-3 (Table 3). A total volume of 2 L of culture media was obtained after growth (8 × 250 mL in 500 mL Schott flasks). The medium was filtered through Celite and adsorbed onto a C<sub>18</sub> reversed-phase cartridge (10 g) using a peristaltic pump. The eluents used were 75:25, 50:50, and 25:75 H<sub>2</sub>O/MeOH and 100% MeOH. After evaporation, fraction 100% MeOH contained metabolites **3** and **4**, detected by HPLC-PDA-MS analysis, as well as citrinalins A (**5**) and B (**6**), identified after their isolation (see below). This fraction was purified using HPLC with a C<sub>18</sub> reversed-phase column (Inertsil ODS-3, 250 × 4.6 mm; 5 μm) and 70:30 MeOH/H<sub>2</sub>O as eluent during a total run time of 30 min and a flow rate of 1.0 mL/min. The major compounds isolated were identified as (*E*)-1-(2,3-dihydro-1*H*-pyrrol-1-yl)-2-methyldec-8-ene-1,3-dione (**3**) and 1-(2,3-dihydro-1*H*-pyrrol-1-yl)-2-methyldecane-1,3-dione (**4**) by analysis of <sup>1</sup>H, <sup>13</sup>C, <sup>1</sup>H–<sup>1</sup>H COSY, HSQC, HMBC, and ESIMS data and comparison with literature data.<sup>54–56</sup>

**Isolation of Compounds **5** and **6**.** *P. citrinum* was first grown using the following F53-OPTIMUM-3 growth conditions (Table 4). The growth medium was filtered, adsorbed onto a C<sub>18</sub> cartridge (10 g), and eluted with 100% H<sub>2</sub>O (discarded), 25:75 MeOH/H<sub>2</sub>O (fraction 1), 50:50 MeOH/H<sub>2</sub>O (fraction 2), 75:25 MeOH/H<sub>2</sub>O (fraction 3), and 100% MeOH (fraction 4). Fraction 4 was subjected to a HPLC separation using a reversed-phase C<sub>18</sub> Inertsil ODS-3 column (250 × 4.6 mm, 5 μm) using 60:40 MeOH/H<sub>2</sub>O at 1.0 mL/min, to give 0.6 mg of impure citrinalin A (**5**). A subsequent growth experiment using the F53-OPTIMUM-3 growth conditions, but for 28 days, yielded 1.7 mg of a mixture of **5** and **6** after a separation using the previous HPLC conditions. This mixture was separated by reversed-phase HPLC using a C<sub>18</sub> Inertsil ODS-3 column (250 × 4.6 mm, 5 μm) with 11:9 (0.05% TFA/H<sub>2</sub>O)/MeOH as eluent to give a pure sample of citrinalin A (**5**) (0.8 mg) and 0.4 mg of citrinalin B (**6**).

**Optimization of Growth Culture Conditions for the Production of Alkaloids **5** and **6**.** A third growth experiment for the production of **5** and **6** was tested and compared to the growth under standard conditions after reanalysis of Table S2 considering the chromatographic peak area assigned to citrinalin A (**5**). This reanalysis led us to establish experiment #12 as an improved condition for its production, changing only the temperature from 15 °C to 30 °C. The optimal condition for the production of **6** was named F53-OPTIMUM-4 and established as follows: ASW [salts] = 20%, [nutrients] = 10%, 28 days of incubation, pH 6.0, and temperature of incubation = 30 °C. The regrowth of *P. citrinum* (a) using a standard condition in unchanged MF medium; (b) in a nonoptimized condition, and (c) under the optimized condition F53-OPTIMUM-4 yielded fractions containing compounds **3**, **4**, **5**, **6**, and **9**, as shown in the chromatograms of Figure 5. After SPE of fraction F4 obtained after a new 2 L growth experiment using the F53-

OPTIMUM-4 condition, citrinalin B (**6**) was found to be in this sample, but not citrinalin A (**5**). Compound **6** was purified using the 3:2 (0.05% TFA/H<sub>2</sub>O)/MeOH conditions, to yield 3.8 mg.

**Citrinalin A TFA Salt (**5**):** pale yellow crystals; [α]<sub>D</sub><sup>25</sup> +63.1 (c 0.53, MeOH); UV (11:9 (0.05% TFA/H<sub>2</sub>O)/MeOH) λ<sub>max</sub> (log ε) 208 (3.9), 231 (3.8), 261 (3.7), 280 (sh), 355 (3.3) nm; <sup>1</sup>H NMR, see Table 7; <sup>13</sup>C NMR, see Table 7; <sup>15</sup>N NMR, see Table 7; (+)-HRESIMS [M + H]<sup>+</sup> *m/z* 454.2362 (calcd for C<sub>25</sub>H<sub>32</sub>N<sub>3</sub>O<sub>5</sub>, 454.2342).

**Citrinalin B TFA Salt (**6**):** pale yellow oil; [α]<sub>D</sub><sup>25</sup> +58.6 (c 2.53, MeOH); UV (3:2 (0.05% TFA/H<sub>2</sub>O)/MeOH) λ<sub>max</sub> (log ε) 208 (3.9), 227 (3.8), 261 (3.7), 280 (sh), 355 (3.3) nm; <sup>1</sup>H NMR, see Table 7; <sup>13</sup>C NMR, see Table 7; <sup>15</sup>N NMR, see Table 7; (+)-HRESIMS [M + H]<sup>+</sup> *m/z* 454.2354 (calcd for C<sub>25</sub>H<sub>32</sub>N<sub>3</sub>O<sub>5</sub>, 454.2342).

**X-ray Crystallographic Analysis of Citrinalin A (**5**).** Colorless crystals of **5** were obtained in MeOH. Crystal data were obtained on a Bruker APEX DUO single-crystal diffractometer with graphite-monochromated Cu Kα radiation (λ = 1.54178 Å) and collected using both ω and φ scan modes, with a combination of 20 and 60 s exposures. The structure was solved by direct methods<sup>61</sup> and refined using full-matrix least-squares difference Fourier techniques.<sup>62</sup> The material crystallizes with four independent molecules in the asymmetric unit, in addition to four trifluoroacetate molecules and four H<sub>2</sub>O molecules. Nitrogen N20 on each molecule is protonated and associated with a TFA anion. Two of the molecules are disordered and were modeled in two orientations. Most NH hydrogens were located in difference maps and refined isotropically; however H3B, H3D, and H20B could not be refined and were thus placed in calculated positions. All CH hydrogen atoms were placed in calculated positions. The absolute configuration was determined on the basis of the refined Flack parameter.<sup>63</sup>

**Time-Course Experiment of *P. citrinum*.** After initial growth of *P. citrinum* in Petri dishes, 10<sup>5</sup> spores/mL were inoculated in 50 mL of growth medium in 250 mL Erlenmeyer flasks, in a duplicate experiment. Growth conditions were the same as those for F53-OPTIMUM-3. The growth medium was harvested each day, over 40 days, as follows. The liquid medium was filtered through a 1 cm Celite pad. The filtered medium was subjected to a SPE with 100% H<sub>2</sub>O, 50:50 H<sub>2</sub>O/MeOH (fraction 1), and 100% MeOH (fraction 2). The 100% H<sub>2</sub>O fraction was partitioned against EtOAc. Fraction 1, fraction 2, and the EtOAc extract of the aqueous fraction were all evaporated to dryness and weighed. Two-milligram aliquots of all fractions obtained each day of the time-course experiment were then subjected to HPLC-PDA-MS analysis. HPLC conditions: column, C<sub>18</sub> X-Terra (50 × 2.1 mm; 3.5 μm pore); eluent, a gradient of 1:1 MeOH/MeCN in H<sub>2</sub>O, starting at 10/90 to 100% 1:1 MeOH/MeCN in 12 min, remaining in the 100% organic solvent mixture until 16 min, then back to the initial conditions after 23 min; flow rate, 0.5 mL/min. PDA at λ<sub>max</sub> 254. The relative amount of each metabolite was normalized in molar concentrations using the Beer–Lambert law.

**Antimycobacterial Activity against *M. tuberculosis* H37Rv.** The procedure for this assay has been previously reported.<sup>64</sup>

**Antimicrobial Activity.** The bacterial and fungal isolates used in this study were methicillin-resistant *Staphylococcus aureus*, *Escherichia coli*, *Pseudomonas aeruginosa*, and *Candida albicans*. The *in vitro* susceptibility of each compound was determined by the broth microdilution method according to the guidelines by the National Committee for Clinical Laboratory Standards.<sup>65</sup> Briefly, 2-fold serial dilutions of compounds were prepared in 96-well microtiter plates from stock solutions in an RPMI-1640 broth medium buffered to a final pH of 7.5 with 0.165 M morpholinepropanesulfonic acid to a final volume of 100 μL. Kanamycin and polymyxin B were used as controls. The final drug concentrations tested were from 0.5 to 128 μg/mL. Bacterial inocula were prepared from 24 h cultures on Tryptic soy agar plates at 37 °C. The inocula were obtained by harvesting colonies into a sterile saline tube and diluted into RPMI-1640 broth medium to yield a final inoculum concentration of 2 × 10<sup>3</sup> cells per mL. The microdilution wells, which contained 100 μL of the serially diluted compound, were inoculated with 100 μL of the resulting bacterial suspension. The final inoculum concentration after dilution with the drug suspension was 10<sup>3</sup>/10<sup>4</sup> cells per mL. Four wells containing the drug-free medium, DMSO, and inoculum were used as controls. The inoculated plates were incubated at 37 °C for 24 h. The growth was determined by the OD at 600 nm using a DTX 880 (Beckman Coulter Inc.) plate reader. The MIC end point was defined as the lowest concentration with complete (90%) growth inhibition.

**Cytotoxicity Assessment.** Cellular responses of human breast carcinoma (ATCC #HTB-129) with the treatment of the compounds were analyzed by MTT assay (MTT: thiazolyl blue tetrazolium bromide, Sigma-Aldrich). Cell cultures were prepared by incubating the cell line in Falcon BD T-25 vented tissue culture flasks. Media were renewed two times weekly, and cells were subcultured when they became confluent. All cell culture reagents were purchased from Invitrogen. The human breast carcinoma cells were grown in Leibovitz's L-15 medium with 2 mM L-glutamine, supplemented with insulin 0.01 mg/mL, FBS 10%, penicillin 50 IU/mL, and streptomycin 50 µg/mL at 37 °C with atmospheric air.

**Cell Viability Assay.** Cell viability assay was performed in flat-bottom plates (Becton Dickinson, Franklin Lakes, NJ). The cells were resuspended in fresh culture medium at a density of  $1 \times 10^5$  cells/mL. An aliquot of 100 µL of cell suspension was added to wells in columns 3 through 11. Culture medium (200 µL) was added to wells in column 2 ("blank"), and 200 µL of sterile distilled water was added to the plate's outer wells to prevent evaporation. Each plate was incubated for 24 h before treatment with the compounds. Compounds were dissolved in DMSO, serially diluted in culture medium in concentrations from 200 to 1.76 µg/mL, and added to the wells in columns 4 through 11. For "no treatment" control 100 µL of culture medium was added to the wells in column 3. For the "DMSO effect" control 100 µL of 1% DMSO was added to the wells in column 4. The plate was incubated for 72 h. Then 50 µL of MTT solution (2.5 mg/mL) was added to all of the plate's experimental wells, except those containing water. The plate was incubated for 3 h and then spun on an IEC HN-S II centrifuge at low speed for 2 min. An aliquot of 230 µL of medium was carefully aspirated from each well. DMSO (150 µL) was added to lyse the cells and solubilize the crystals. The plate was placed on an Orbit P4 shaker for 3 min (Labnet International, Woodbridge, NJ) to dissolve the formazan crystals. The samples were read on a DTX 880 (Beckman Coulter Inc.) plate reader at a wavelength of 570 nm. Cell viability at each drug concentration was expressed as a percentage of untreated controls, and IC<sub>50</sub> values were determined using Prism5 (GraphPad, San Diego, CA, USA).

**Acknowledgment.** The authors thank Prof. E. R. P. Filho (Departamento de Química, Universidade Federal de São Carlos) for fruitful discussions on the experimental design statistical analysis, as well as the administrative and technical staff of Centro de Biologia Marinha of Universidade de São Paulo, for providing many facilities during fieldwork. Financial support by FAPESP as BIOTA/BIOprospecTA grant 05/60175-2 to R.G.S.B. and a scholarship to E.F.P. (06/61693-0) is gratefully acknowledged.

**Supporting Information Available:** Fractional factorial experiment design matrices for the growth of *P. oxalicum* and *P. citrinum*, procedures for fungal strain identification, procedure for experimental design statistical analysis, crystal data for citrinalin A, ORTEP diagram for citrinalin A, <sup>1</sup>H and <sup>13</sup>C NMR spectra of citrinalins A and B. This material is available free of charge via the Internet at <http://pubs.acs.org>.

## References and Notes

- Adrio, J. L.; Demain, A. L. *Int. Microbiol.* **2003**, *6*, 191–199.
- Demain, A. L. *Appl. Microbiol. Biotechnol.* **1999**, *52*, 455–463.
- Demain, A. L. *Biotechnol. Adv.* **2000**, *18*, 499–514.
- Martin, J. F. J. *Bacteriol.* **2000**, *182*, 2355–2362.
- Penalva, M. A.; Rowlands, R. T.; Turner, G. *Trends Biotechnol.* **1998**, *16*, 483–489.
- Bentley, R. *Nat. Prod. Rep.* **2006**, *23*, 1046–1062.
- Burdock, F. A.; Soni, M. G.; Carabin, I. G. *Reg. Toxicol. Pharmacol.* **2001**, *33*, 80–101.
- Bode, H. B.; Bethe, B.; Höfs, R.; Zeeck, A. *ChemBioChem* **2002**, *3*, 619–627.
- Prathumpai, W.; Kocharin, K.; Phimmakong, K.; Wongsap, P. *Appl. Biochem. Biotechnol.* **2007**, *126*, 223–232.
- Bugni, T. S.; Ireland, C. M. *Nat. Prod. Rep.* **2004**, *21*, 143–163.
- Büchls, J. *Biochem. Eng. J.* **2001**, *7*, 91–98.
- Feng, K.-C.; Rou, T.-M.; Liu, B.-L.; Tzeng, Y.-M.; Chang, Y.-N. *Enzyme Microb. Technol.* **2004**, *34*, 22–25.
- Beppu, T. *Tibtech* **1995**, *13*, 264–269.
- Calvo, A. M.; Wilson, R. A.; Bok, J. W.; Keller, N. P. *Microbiol. Mol. Biol. Rev.* **2002**, *66*, 447–459.
- Yu, J. H.; Keller, N. *Ann. Rev. Phytopathol.* **2005**, *43*, 437–458.
- Parekh, S.; Vinci, V. A.; Strobel, R. J. *Appl. Microbiol. Biotechnol.* **2000**, *54*, 287–301.
- Balaraman, K.; Mathew, N. *Indian J. Med. Res.* **2006**, *123*, 525–530.
- Dong, C. H.; Yao, Y. J. *J. Appl. Microbiol.* **2005**, *99*, 483–492.
- Jackson, M. A. *J. Ind. Microbiol. Biotechnol.* **1997**, *19*, 180–187.
- Petersen, F.; Moerker, T.; Vanzanella, F.; Peter, H. H. *J. Antibiot.* **1994**, *47*, 1098–1103.
- Zhu, M.; Yu, L. J.; Li, W.; Zhou, P. P.; Li, C. Y. *Enz. Microb. Technol.* **2006**, *38*, 735–740.
- Cihangir, N.; Sarikaya, E. *World J. Microbiol. Biotechnol.* **2004**, *20*, 193–197.
- Mendes, L. F.; Bastos, E. L.; Desjardin, D. E.; Stevani, C. V. *FEMS Microbiol. Lett.* **2008**, *282*, 132–139.
- Hölker, U.; Höfer, M.; Lenz, J. *Appl. Microbiol. Biotechnol.* **2004**, *64*, 175–186.
- Jing, D. B.; Li, P. J.; Stagnitti, F.; Xiong, X. Z. *Can. J. Microbiol.* **2007**, *53*, 245–251.
- Revankar, M. S.; Desai, K. M.; Lele, S. S. *Appl. Biochem. Biotechnol.* **2007**, *143*, 16–26.
- Song, X. Y.; Xie, S. T.; Chen, X. L.; Sun, C. Y.; Shi, M.; Zhang, Y. Z. *J. Biotechnol.* **2007**, *131*, 209–215.
- Cueto, M.; Jensen, P. R.; Kauffman, C.; Fenical, W.; Lobkovsky, E.; Clardy, J. *J. Nat. Prod.* **2001**, *64*, 1444–1446.
- Oh, D. C.; Jensen, P. R.; Kauffman, C. A.; Fenical, W. *Bioorg. Med. Chem.* **2005**, *13*, 5267–5273.
- Oh, D.-C.; Kauffman, C. A.; Jensen, P. R.; Fenical, W. *J. Nat. Prod.* **2007**, *70*, 515–520.
- Wang, X. J.; Bai, J. G.; Liang, Y. X. *Appl. Microbiol. Biotechnol.* **2007**, *73*, 533–540.
- Slatery, M.; Rajbhandari, I.; Wesson, K. *Microb. Ecol.* **2001**, *41*, 90–96.
- Lim, J. S.; Park, M. C.; Lee, J. H.; Park, S. W.; Kim, S. W. *Eur. Food Res. Technol.* **2005**, *221*, 639–644.
- Ooijskaas, L. P.; Wilkinson, E. C.; Tramper, J.; Buitelaar, R. M. *Biotechnol. Bioeng.* **1999**, *64*, 92–100.
- Rispoli, F. J.; Shah, V. J. *Ind. Microbiol. Biotechnol.* **2007**, *34*, 349–355.
- Shi, L. E.; Ying, G. Q.; Zhang, X. Y.; Tang, Z. X.; Chen, J. S.; Xiong, W. Y.; Liu, H. Z. *Food Technol. Biotechnol.* **2007**, *45*, 126–133.
- Cockshott, A. R.; Sullivan, G. R. *Proc. Biochem.* **2001**, *36*, 647–660.
- Chakravarti, R.; Sahai, V. *Proc. Biochem.* **2002**, *38*, 481–486.
- Furtado, N. A. J. C.; Duarte, M. C. T.; Albuquerque, S.; Mello, C.; Bastos, J. K. *Microbiol. Res.* **2005**, *160*, 141–148.
- Sayyad, S. A.; Panda, B. P.; Javed, S.; Ali, M. *Appl. Microbiol. Biotechnol.* **2007**, *73*, 1054–1058.
- Tully, T. P.; Bergum, J. S.; Schwarz, S. R.; Durand, S. C.; Howell, J. M.; Patel, R. N.; Cino, P. M. *J. Ind. Microbiol. Biotechnol.* **2007**, *34*, 193–202.
- Li, Y.; Cui, F.; Liu, F.; Liu, Z.; Xu, Y.; Zhao, H. *Enz. Microb. Technol.* **2007**, *40*, 1381–1388.
- Li, Y.; Liu, Z.; Cui, F.; Xu, Y.; Zhao, H.; Liu, Z. *J. Food Sci.* **2007**, *72*, E320–E329.
- For a review, see: Kennedy, M.; Krouse, D. *J. Ind. Microb. Biotechnol.* **1999**, *23*, 456–475.
- Vita-Marques, A. M.; Lira, S. P.; Berlink, R. G. S.; Seleguim, M. H. R.; Sponchiado, S. R. P.; Tauk-Tornisiolo, S. M.; Barata, M.; Pessoa, C.; Moraes, M. O.; Coelho, B.; Nascimento, G. G. F.; Souza, A. O.; Minarini, P. R. R.; Silva, C. L.; Silva, M.; Pimenta, E. F.; Thiemann, O.; Passarini, M. R. Z.; Sette, L. D. *Quím. Nova* **2008**, *31*, 1099–1103.
- Yang, L. H.; Miao, L.; Lee, O. O.; Li, X.; Xiong, H.; Pang, K.-L.; Vrijmoed, L.; Qian, P.-Y. *Appl. Microbiol. Biotechnol.* **2007**, *74*, 1221–1231.
- Madla, S.; Kittakoop, P.; Wongsap, P. *Let. Appl. Microbiol.* **2006**, *43*, 548–553.
- Nielsen, K. F.; Smedsgaard, J. *J. Chromatogr. A* **2003**, *1002*, 111–136.
- Nagel, D. W.; Pachler, K. G. R.; Steyn, P. S.; Vleggaar, R.; Wessels, P. L. *Tetrahedron* **1976**, *32*, 2625–2631.
- Nozawa, K.; Nakajima, S. *J. Nat. Prod.* **1979**, *42*, 374–377.
- Konda, Y.; Onda, M.; Hirano, A.; Omura, S. *Chem. Pharm. Bull.* **1980**, *28*, 2987–2993.
- Hirano, A.; Iwai, Y.; Masuma, R.; Tei, K.; Omura, S. *J. Antibiot.* **1979**, *32*, 781–785.
- Koizumi, Y.; Arai, M.; Tomoda, H.; Omura, S. *Biochim. Biophys. Acta* **2004**, *1693*, 47–55.
- Cantín, A.; Moya, P.; Castillo, M. A.; Primo, J.; Miranda, M. A.; Primo-Yúfera, E. *Eur. J. Org. Chem.* **1999**, 221–226.
- Moya, P.; Cantín, A.; Castillo, M. A.; Primo, J.; Miranda, M. A.; Primo-Yúfera, E. *J. Org. Chem.* **1988**, *63*, 8530–8535.
- Castillo, M. A.; Moya, P.; Cantín, A.; Miranda, M. A.; Primo, J.; Hernández, E.; Primo-Yúfera, E. *J. Agric. Food Chem.* **1999**, *47*, 2120–2124.
- Crystallographic data for the structure of citrinalin A (5) herein reported have been deposited with the Cambridge Crystallographic Data Centre

- (assessment number 782921). Copies of the data can be obtained, free of charge, on application to the Director, CCDC, 12 Union Road, Cambridge CB2 1EZ, UK (fax: +44-(0)1223-336033 or e-mail: deposit@ccdc.cam.ac.uk).
- (58) Bond, R. F.; Boeyens, J. C. A.; Holzapfel, C. W.; Steyn, P. S. *J. Chem. Soc., Perkin Trans. 1* **1979**, 1751–1761.
- (59) Steyn, P. S.; Vlegaar, R.; Rabies, C. J. *Phytochemistry* **1981**, *20*, 538–539.
- (60) Li, Y.; Liu, Z.; Zhao, H.; Xu, Y.; Cui, F. *Biochem. Eng. J.* **2007**, *34*, 82–86.
- (61) Altomare, A.; Burla, M. C.; Camalli, M.; Cascarano, G. L.; Giacomazzo, C.; Guagliardi, A.; Moliterni, A. G. G.; Polidori, G.; Spagna, R. *J. Appl. Crystallogr.* **1999**, *32*, 115–119.
- (62) *SHELXTL Version 2008/4*; Bruker AXS Inc.: Madison, WI, USA, 2008.
- (63) (a) Flack, H. D. *Acta Crystallogr., Sect. A* **1983**, *39*, 876–881. (b) Bernardinelli, G.; Flack, H. D. *Acta Crystallogr., Sect. A* **1985**, *41*, 500–511.
- (64) Oliveira, M. F.; Oliveira, J. H. H. L.; Galetti, F. C. S.; Souza, A. O.; Silva, C. L.; Hajdu, E.; Peixinho, S.; Berlinck, R. G. S. *Planta Med.* **2006**, *72*, 437–441.
- (65) National Committee for Clinical Laboratory Standards. 2002. Reference method for broth dilution antifungal susceptibility testing of yeast, 2nd ed. Approved standard M27-A2. National Committee for Clinical Laboratory Standards, Wayne, PA, USA.

NP100470H